

An Antilock Molecular Braking System

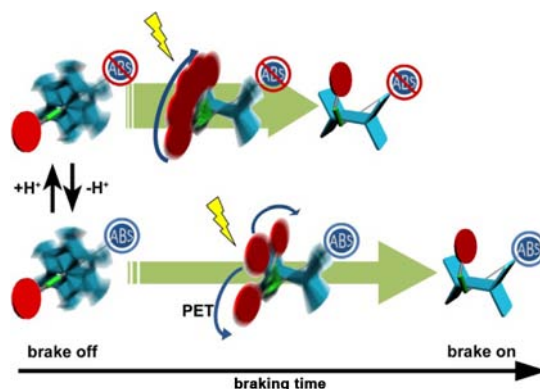
Wei-Ting Sun,[†] Shou-Ling Huang,[†] Hsuan-Hsiao Yao,[‡] I-Chia Chen,^{*,‡} Ying-Chih Lin,[†]
and Jye-Shane Yang^{*,†}

Department of Chemistry, National Taiwan University, Taipei, Taiwan 10617, and
Department of Chemistry, National Tsing Hua University, Hsinchu, Taiwan 30013

icchen@mx.nthu.edu.tw; jsyang@ntu.edu.tw

Received July 3, 2012

ABSTRACT



A light-driven molecular brake displaying an antilock function is constructed by introducing a nonradiative photoinduced electron transfer (PET) decay channel to compete with the trans (brake-off) \rightarrow cis (brake-on) photoisomerization. A fast release of the brake can be achieved by deactivating the PET process through addition of protons. The cycle of irradiation–protonation–irradiation–deprotonation conducts the brake function and mimics the antilock braking system (ABS) of vehicles.

Photoinduced electron transfer (PET) plays a crucial role in both biological and chemical systems. In photosynthetic reaction centers,¹ cascade PET converts the photon energy

to chemical energy. In photovoltaic devices,² PET leads to charge separation and creates electric power. Many intensity-based photoluminescent sensors rely on PET to quench the excited state.³ For molecular devices, PET could drive a linear or rotary motion.⁴ We demonstrate herein a new application of PET, namely, to perform an antilock function in photon-driven molecular brakes that mimics the antilock braking system (ABS) equipped in vehicles.

The development of molecular machinery systems is an important subject in nanoscience and nanotechnology.⁵ Effective control of linear or rotary molecular motions is a prerequisite toward artificial molecular machines.⁶ Many prototypes of controlled motions on the molecular level

[†]National Taiwan University.

[‡]National Tsing Hua University.

(1) (a) Wasielewski, M. R. *Chem. Rev.* **1992**, *92*, 435–461. (b) Heller, B.; Holten, D.; Kirmaier, C. *Science* **1995**, *269*, 940–945.

(2) (a) Mishra, A.; Fischer, M. K. R.; Bäuerle, P. *Angew. Chem., Int. Ed.* **2009**, *48*, 2474–2499. (b) Facchetti, A. *Chem. Mater.* **2010**, *23*, 733–758. (c) Yella, A.; Lee, H.-W.; Tsao, H. N.; Yi, C.; Chandiran, A. K.; Nazeeruddin, M. K.; Diau, E. W.-G.; Yeh, C.-Y.; Zakeeruddin, S. M.; Grätzel, M. *Science* **2011**, *334*, 629–634.

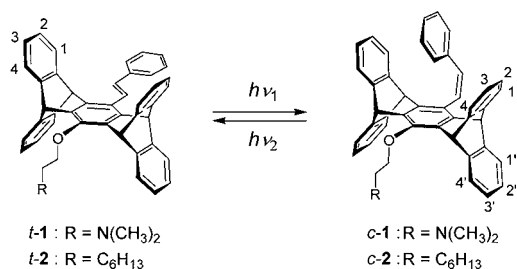
(3) (a) Thomas, S. W., III; Joly, G. D.; Swager, T. M. *Chem. Rev.* **2007**, *107*, 1339–1386. (b) Lodeiro, C.; Capelo, J. L.; Mejuto, J. C.; Oliveira, E.; Santos, H. M.; Pedras, B.; Nuñez, C. *Chem. Soc. Rev.* **2010**, *39*, 2948–2976. (c) Kobayashi, H.; Ogawa, M.; Alford, R.; Choyke, P. L.; Urano, Y. *Chem. Rev.* **2010**, *110*, 2620–2640.

(4) (a) Ballardini, R.; Balzani, V.; Gandolfi, M. T.; Prodi, L.; Venturi, M.; Philp, D.; Ricketts, H. G.; Stoddart, J. F. *Angew. Chem., Int. Ed.* **1993**, *32*, 1301–1303. (b) Ashton, P. R.; Ballardini, R.; Balzani, V.; Boyd, S. E.; Credi, A.; Gandolfi, M. T.; Gómez-López, M.; Iqbal, S.; Philp, D.; Preece, J. A.; Prodi, L.; Ricketts, H. G.; Stoddart, J. F.; Tolley, M. S.; Venturi, M.; White, A. J. P.; Williams, D. J. *Chem.—Eur. J.* **1997**, *3*, 152–170. (c) Livoreil, A.; Sauvage, J.-P.; Armaroli, N.; Balzani, V.; Flamigni, L.; Ventura, B. *J. Am. Chem. Soc.* **1997**, *119*, 12114–12124. (d) Panman, M. R.; Bodis, P.; Shaw, D. J.; Bakker, B. H.; Newton, A. C.; Kay, E. R.; Brouwer, A. M.; Buma, W. J.; Leigh, D. A.; Woutersen, S. *Science* **2010**, *328*, 1255–1258.

(5) (a) Kottas, G. S.; Clarke, L. I.; Horinek, D.; Michl, J. *Chem. Rev.* **2005**, *105*, 1281–1376. (b) Kinbara, K.; Aida, T. *Chem. Rev.* **2005**, *105*, 1377–1400. (c) Kay, E. R.; Leigh, D. A.; Zerbetto, F. *Angew. Chem., Int. Ed.* **2007**, *46*, 72–191. (d) Saha, S.; Stoddart, J. F. *Chem. Soc. Rev.* **2007**, *36*, 77–92. (e) Feringa, B. L. *J. Org. Chem.* **2007**, *72*, 6635–6652. (f) Balzani, V.; Credi, A.; Venturi, M. *Molecular Devices and Machines: Concepts and Perspectives for the Nanoworld*; Wiley-VCH: 2008.

(6) (a) Champin, B.; Mobian, P.; Sauvage, J.-P. *Chem. Soc. Rev.* **2007**, *36*, 358–366. (b) Bonnet, S.; Collin, J.-P. *Chem. Soc. Rev.* **2008**, *37*, 1207–1217. (c) Feringa, B. L.; van Delden, R. A.; ter Wiel, M. K. J. *Pure Appl. Chem.* **2003**, *75*, 563–575.

Scheme 1. Trans–Cis Photoisomerization of **1** and **2**^a



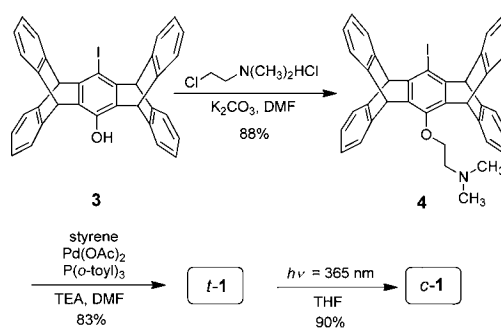
^aThe numeric labels for protons and carbons are for discussion of the NMR spectra.

have been reported and dubbed as shuttles, elevators, brakes, and many others, in analogy to the operation of the corresponding macroscopic objects.^{5,7–10} The energy sources (fuels) for the operation are versatile, including chemicals, light (photons), and electric or thermal energy. A combination of different energy sources could improve the operation efficiency⁸ and/or perform multiple motion control⁹ or functions.¹⁰ We report herein a photon-driven molecular brake (**1**) having a proton-gated antilock function; namely, the brake performance is driven by UV light, but the brake operation is gated by the proton-responsive amino group (Scheme 1).

The antilock braking system **1** was designed from the recently reported photon-gated molecular brake **2**.¹¹ The trans and cis forms of **2** ($t\text{-2}$ and $c\text{-2}$) correspond to the brake-off and brake-on states with a rotation rate of 10⁹ and 10² s⁻¹, respectively, for the pentiptycene rotor at room temperature. The 10⁷-fold braking effect can be further improved by increasing the size of the styryl brake component through adding bulky substituents to the phenyl group.¹¹ The brake operation is also effective, as the switching from the brake-off ($t\text{-2}$) to the brake-on ($c\text{-2}$) state is nearly quantitative. Since the photoinduced trans → cis isomerization is operating the brake function, the presence of other competing nonradiative decay

channels could dynamically abort the isomerization and thus increase the braking time. This phenomenon resembles the ABS function that increases the braking distance for vehicles on loose surfaces.¹² To prove this concept, we have introduced an amino group as in **1** to invoke a nonradiative PET process to the electronically excited state of the stilbene moiety, given the fact that a tertiary amino group is a potential electron donor for excited stilbenes.¹³ The PET process could compete but not inhibit the isomerization reaction of the brake-off state ($t\text{-1}$) toward the brake-on ($t\text{-1}$) state so that formation of a complete brake state is delayed. Such a PET-based ABS function could in principle be deactivated by protonation of the amino group to perform the simple brake function as in the case of **2**.

Scheme 2. Synthesis of $t\text{-1}$ and $c\text{-1}$



The synthesis of **1** is shown in Scheme 2. The known compound iodo-substituted pentiptycene phenol **3**¹⁴ underwent a typical S_N2 reaction with the hydrochloride salt of 2-chloro-*N,N*-dimethyl-ethylamine¹⁵ to afford **4** in an excellent yield (88%). The trans isomer of **1** ($t\text{-1}$) was then prepared from the Heck reaction between styrene and **4**. The cis isomer $c\text{-1}$ was obtained on irradiation of $t\text{-1}$ in THF at 365 nm.

The rotational barriers and activation parameters for the pentiptycene rotor in $c\text{-1}$ have been evaluated by variable-temperature (VT) NMR spectroscopy. Detailed VT NMR spectra (Figures S1–S5) and peak assignments are supplied as Supporting Information. The rate constant

(7) (a) Setaka, W.; Nirengi, T.; Kabuto, C.; Kira, M. *J. Am. Chem. Soc.* **2008**, *130*, 15762–15763. (b) Yang, J.-S.; Huang, Y.-T.; Ho, J.-H.; Sun, W.-T.; Huang, H.-H.; Lin, Y.-C.; Huang, S.-J.; Huang, S.-L.; Lu, H.-F.; Chao, I. *Org. Lett.* **2008**, *10*, 2279–2282. (c) Coskun, A.; Friedman, D. C.; Li, H.; Patel, K.; Khatib, H. A.; Stoddart, J. F. *J. Am. Chem. Soc.* **2009**, *131*, 2493–2495. (d) Crowley, J. D.; Hänni, K. D.; Leigh, D. A.; Slawin, A. M. Z. *J. Am. Chem. Soc.* **2010**, *132*, 5309–5314. (e) Leblond, J.; Gao, H.; Petitjean, A.; Leroux, J.-C. *J. Am. Chem. Soc.* **2010**, *132*, 8544–8545. (f) Basheer, M. C.; Oka, Y.; Mathews, M.; Tamaoki, N. *Chem.—Eur. J.* **2010**, *16*, 3489–3496. (g) Yang, C.-H.; Prabhakar, C.; Huang, S.-L.; Lin, Y.-C.; Tan, W. S.; Misra, N. C.; Sun, W.-T.; Yang, J.-S. *Org. Lett.* **2011**, *13*, 5632–5635.

(8) Chen, Y.-C.; Sun, W.-T.; Lu, H.-F.; Chao, I.; Huang, G.-J.; Lin, Y.-C.; Huang, S.-L.; Huang, H.-H.; Lin, Y.-D.; Yang, J.-S. *Chem.—Eur. J.* **2011**, *17*, 1193–1200.

(9) (a) Zhang, D.; Zhang, Q.; Su, J. H.; Tian, H. *Chem. Commun.* **2009**, 1700–1702. (b) Ruangsupapichat, N.; Pollard, M. M.; Harutyunyan, S. R.; Feringa, B. L. *Nat. Chem.* **2011**, *3*, 53–60.

(10) (a) Wang, Q.-C.; Qu, D.-H.; Ren, J.; Chen, K.; Tian, H. *Angew. Chem., Int. Ed.* **2004**, *43*, 2661–2665. (b) Qu, D. H.; Feringa, B. L. *Angew. Chem., Int. Ed.* **2010**, *49*, 1107–1110.

(11) Sun, W.-T.; Huang, Y.-T.; Huang, G.-J.; Lu, H.-F.; Chao, I.; Huang, S.-L.; Huang, S.-J.; Lin, Y.-C.; Ho, J.-H.; Yang, J.-S. *Chem.—Eur. J.* **2010**, *16*, 11594–11604.

(12) (a) Mollenhauer, M. A.; Dingus, T. A.; Carney, C.; Hankey, J. M.; Jahns, S. *Accident Anal. Prev.* **1997**, *29*, 97–108. (b) Forkenbrock, G.; Flick, M.; Garrott, W. R. *Warrendale, PA: Society of Automotive Engineers* **1999**, 1999-01-1287.

(13) (a) Hub, W.; Schneider, S.; Dörr, F.; Oxman, J. D.; Lewis, F. D. *J. Am. Chem. Soc.* **1984**, *106*, 708–715. (b) Ho, T.-I. *J. Photochem. Photobiol., A* **1998**, *112*, 159–164. (c) Lewis, F. D.; Kultgen, S. G. *J. Photochem. Photobiol., A* **1998**, *112*, 159–164. (d) Buruiana, E. C.; Zamfir, M.; Buruiana, T. *Eur. Polym. J.* **2007**, *43*, 4316–4324.

(14) Yang, J.-S.; Yan, J.-L.; Jin, Y.-X.; Sun, W.-T.; Yang, M.-C. *Org. Lett.* **2009**, *11*, 1429–1432.

(15) Fornasier, R.; Scrimin, P.; Tecilla, P.; Tonellato, U. *J. Am. Chem. Soc.* **1989**, *111*, 224–229.

(16) (a) Saltiel, J.; Sun, Y.-P. In *Photochromism, Molecules and Systems*; Dürr, H.; Bouas-Laurent, H., Eds.; Elsevier: Amsterdam, 1990; pp 64–164. (b) Waldeck, D. H. *Chem. Rev.* **1991**, *91*, 415–436. (c) Görner, H.; Kuhn, H. J. *Adv. Photochem.* **1995**, *19*, 1–117. (d) Zimmer, M. In *Cis-Trans Isomerization in Biochemistry*; Dugave, C., Ed.; Wiley-VCH: Weinheim, 2006.

(*k*) of rotation deduced by line shape analysis of the C(1) and C(4) signals of the VT ^{13}C NMR spectra is 670 s^{-1} at 293 K (Figure 1). The *k* value is very close to that (686 s^{-1}) for the parent brake system *c*-2 at 298 K.¹¹ The activation barriers ($E_a = 10.6 \pm 0.6\text{ kcal mol}^{-1}$) and the enthalpy ($\Delta H^\ddagger = 10.1 \pm 0.5\text{ kcal mol}^{-1}$) and entropy ($\Delta S^\ddagger = -11.8 \pm 0.2\text{ cal mol}^{-1}\text{ K}^{-1}$) of activation derived from the Arrhenius and Eyring plots (Figures S6 and S7) also resemble those of *c*-2.¹¹ Evidently, the amino substituent imposes a negligible effect on the rotation kinetics of the pentiptycene rotor. The rotation rate for the pentiptycene rotor in *t*-1 is also expected to be the same as that ($\sim 10^9\text{ s}^{-1}$) in *t*-2, which was evaluated by density functional theory calculations.¹¹ Thus, the braking system 1 retains the excellent performance of 2 with a 10^7 -fold braking effect.

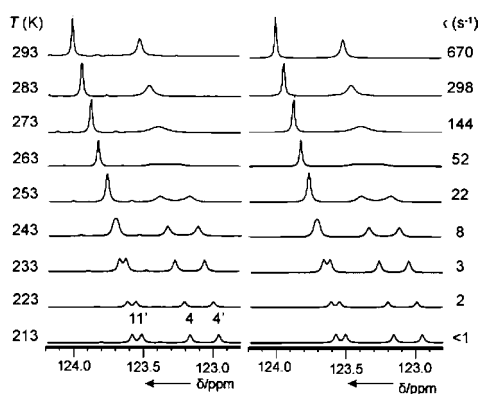


Figure 1. VT ^{13}C NMR (left, 125 MHz) and simulated (right) spectra of *c*-1 in CD_2Cl_2 at the region of C(1) and C(4) (see Scheme 1 for labels). Values of temperature (*T*, K) and inter-conversion rate (*k*, s^{-1}) between the two isoenergetic states (i.e., 180° rotation) are also given for each trace.

The photon-driven brake performance for *t*-1 was conducted in acetonitrile. According to the UV absorption spectra of *t*-1 and *c*-1 (Figure 2a), the wavelength 340 nm is suitable for performing the brake operation, as *c*-1 has little absorptivity at 340 nm. Indeed, the *t*-1 \rightarrow *c*-1 conversion is as high as 95% in the photostationary state. The quantum efficiency for the *t*-1 \rightarrow *c*-1 switching (Φ_{tc}) is 0.11, which is much lower than that (0.48) for the reference system *t*-2 under the same conditions. The difference between *t*-1 and *t*-2 reveals the effect of the amino group on Φ_{tc} . The amino effect is deactivated by protons, as a high Φ_{tc} (0.49) is recovered for *t*-1 in the presence of 10 equiv of HCl. The relative efficiency for the *t*-1 \rightarrow *c*-1 switching is shown in Figure 3a. Whereas complete braking takes more than 175 min in the absence of protons (curve i), it takes ~ 100 min in the presence of protons (curve ii). It should be noted that the presence of protons neither perturbs the absorption profiles of both *t*-1 and *c*-1 (Figure 2a) nor induces the *t*-1 \rightarrow *c*-1 isomerization in the dark (curve iii of Figure 3a). These observations indicate that PET occurs from the amino group to the excited stilbene and is responsible for the antilock function.

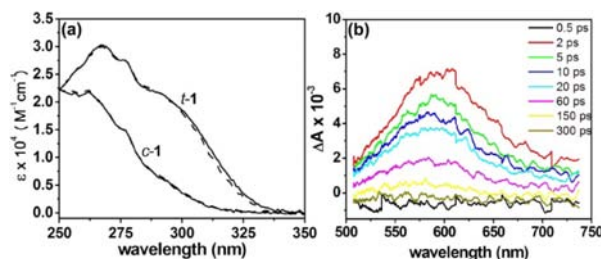


Figure 2. (a) UV absorption spectra of *t*-1 and *c*-1 in the absence (solid lines) and presence (dash lines) of 10 equiv of HCl in acetonitrile, and (b) transient absorption spectra of *t*-1 in acetonitrile at 0.5–300 ps ($\lambda_{\text{ex}} = 266\text{ nm}$).

More information about the PET reaction is obtained from time-resolved spectroscopy. The fluorescence lifetimes (τ_f) for *t*-1 and *t*-2 in acetonitrile are 77 and 88 ps, respectively.¹⁷ Provided that *t*-1 and *t*-2 correspond to the PET and PET-free systems, the rate constant ($k_{\text{PET, intra}}$) for the proposed intramolecular PET is estimated to be $1.6 \times 10^9\text{ s}^{-1}$ (i.e., $(77\text{ ps})^{-1} - (88\text{ ps})^{-1}$). On the basis of Φ_{tc} and τ_f , the rate constants ($k_{\text{tc}} = \Phi_{\text{tc}}/\tau_f$) for the *t*-1 \rightarrow *c*-1 and the *t*-2 \rightarrow *c*-2 conversions are 1.4×10^9 and $5.5 \times 10^9\text{ s}^{-1}$, respectively. The difference in the k_{tc} of *t*-1 vs *t*-2 (i.e., $4.1 \times 10^9\text{ s}^{-1}$) is larger than $k_{\text{PET, intra}}$, which indicates that not only the intramolecular PET but also the intermolecular PET takes place in diminishing the Φ_{tc} . This can be understood by the fact that the measurement of τ_f is in dilute solutions ($1 \times 10^{-5}\text{ M}$) but that of Φ_{tc} is under 100-fold more concentrated solutions. Intermolecular PET between *t*-2 and triethylamine has been investigated. The Stern–Volmer plot (Figure S8) gives rise to a quenching constant of $2.0 \times 10^{10}\text{ s}^{-1}$, indicating a diffusion-controlled PET process.

Another piece of evidence for the occurrence of PET in *t*-1 is provided by the transient absorption spectra. Within 2 ps after excitation of *t*-1 at 266 nm, an absorption band near 600 nm is detected (Figure 2b). The anion radical of the parent *trans*-stilbene was reported to have an absorption maximum near 500 nm.^{13a,18} The absorption maximum is red-shifted for substituted stilbenes.¹⁹ The observed signal for *t*-1 can thus be attributed to the anion radical of the pentiptycene-derived stilbene.

The operation to reverse the brake-on *c*-1 state back to the brake-off *t*-1 state was also investigated. The quantum efficiency for the *c*-1 \rightarrow *t*-1 conversion (Φ_{ct}) is 0.20, which is again lower than 0.37 for the *c*-2 \rightarrow *t*-2 conversion.¹¹ In the presence of 10 equiv of HCl, the Φ_{ct} increases to 0.45. The transient absorption spectra for *c*-1 were also recorded

(17) The fluorescence lifetime is an average of a short major component (62 ps, 92% for *t*-1 and 79 ps, 98% for *t*-2) and a long minor component (250 ps, 8% for *t*-1 and 530 ps, 2% for *t*-2). The distinct lifetimes for the two components are tentatively attributed to conformers of different orientation for the amino group relative to the stilbene chromophore.

(18) Levanon, H.; Neta, P. *Chem. Phys. Lett.* **1977**, *48*, 345–349.

(19) Lewis, F. D.; Wu, T.; Zhang, Y.; Letsinger, R. L.; Greenfield, S. R.; Wasielewski, M. R. *Science* **1997**, *277*, 673–676.

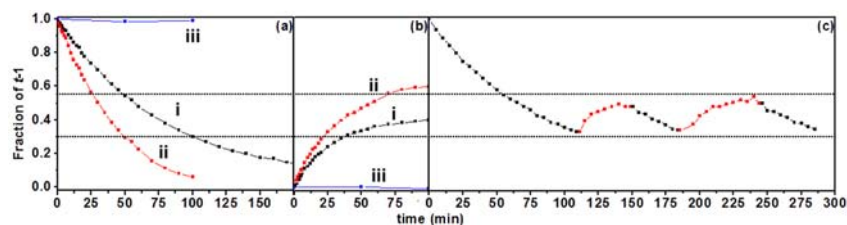
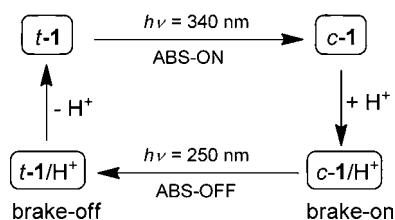


Figure 3. Plots of the fraction of *t-1* against the irradiation time for (a) *t-1* → *c-1* at 340 nm, (b) *c-1* → *t-1* at 250 nm, and (c) *t-1* → *c-1* // *c-1*/H⁺ → *t-1*/H⁺ // *t-1* → *c-1* // *c-1*/H⁺ → *t-1*/H⁺ // *t-1* → *c-1* at alternating 340 and 250 nm in acetonitrile. The substrate concentration is 1.0×10^{-5} M. The black (i) and red (ii) curves are at 0.0 and 10.0 equiv of HCl, respectively, and the blue (iii) curves are at 10.0 equiv of HCl in the dark.

(Figure S9), and the spectral features are similar to the case of *t-1*. Evidently, the PET process observed for *t-1* is also operated in *c-1*, and it could also be deactivated by protonation of the amino group. As depicted in Figure 3b, the relatively longer recovery time for *t-1* in the neutral (curve i) vs the protonated (curve ii) form is consistent with our conclusion. The effective competition of PET to the photoisomerization of *cis*-stilbene observed for the case of *c-1* is rather unusual, given the fact that excited state quenching of *cis*-stilbene due to the torsion of the vinyl C=C is ultrafast (~ 1.3 ps).²⁰ It appears that the bulky pentiptycene group modifies the excited-state potential energy surface for the isomerization process so that the PET process is kinetically compatible. The recovery of *t-1* is $\sim 60\%$ at 250 nm, a wavelength that corresponds to the highest ratio of the molar absorptivity of *c-1* vs *t-1* (Figure 2a). As in the case of *t-1* → *c-1*, protons alone cannot drive the *c-1* → *t-1* isomerization in the dark (Figure 3b, curve iii). Because of the extremely weak fluorescence, no attempts were made to analyze the decay kinetics for *c-1*.

To mimic the ABS operation for the wheels of vehicles, the PET process is desired only in the turn-on but not the turn-off operation of the brake function. In other words, the PET process in *c-1* should be deactivated for a fast recovery of the brake-off *t-1* state. Therefore, an optimal operation of the ABS function can be achieved through the cycle shown in Scheme 3. The fast rotation of the pentiptycene rotor in *t-1* is stopped in *c-1* through the photon (340 nm)-driven ABS operation. Protonation of *c-1* (*c-1*/H⁺) deactivates the ABS function and allows fast photon (250 nm)-induced release of the brake to restore fast rotation of the rotor (*t-1*/H⁺). The ABS function can be turned on again by removing the protons in *t-1*/H⁺ with

Scheme 3. Optimal Operation Procedures for the ABS Function of the Molecular Brake 1



bases. Figure 3c shows 2.5 cycles of Scheme 3 starting from *t-1*. To shorten the experimental time, the photostationary states were not reached for each switching step. Each segment of the curve in Figure 3c is similar to the corresponding segments in Figure 3a and 3b, which is consistent with the expected ABS operation. The operation cycle involves the energy inputs of light, acid (HCl), and base (KO^tBu).

In summary, we report the first example of an antilock molecular braking system operated with photons and chemicals (acids and bases). The antilock function results from the competition of PET with the *cis*–*trans* photoisomerization and can be deactivated with protons. We believe that the rich molecular/supramolecular photochemistry could further improve the function and performance of light-gated molecular devices.

Acknowledgment. We thank the National Science Council of Taiwan for financial support.

Supporting Information Available. Experimental methods, synthesis, 1D and 2D NMR spectra, the Arrhenius and Eyring plots, complete VT ¹³C NMR spectra, and a Stern–Volmer plot. This material is available free of charge via the Internet at <http://pubs.acs.org>.

The authors declare no competing financial interest.

(20) (a) Todd, D. C.; Jean, J. M.; Rosenthal, S. J.; Ruggiero, A. J.; Yang, D.; Fleming, G. R. *J. Chem. Phys.* **1990**, *93*, 8658–8668. (b) Petek, H.; Yoshihara, K.; Fujiwara, Y.; Lin, Z.; Penn, J. H.; Frederick, J. H. *J. Phys. Chem.* **1990**, *94*, 7539–7541.